Electrochemical and Solid-State Letters, **12** (5) J51-J53 (2009)
1099-0062/2009/12(5)/J51/3/$23.00 © The Electrochemical Society

Embedded Optical Sensor Using Gate-Body-Tied Thin-Film Transistor on Low-Temperature Poly-Silicon Display Panel

Wen-Jen Chiang,[z] Chrong-Jung Lin, and Ya-Chin King

National Tsing Hua University, Hsinchu 30013, Taiwan

An embedded photosensor using a gate-body-tied (GBT) thin-film transistor is investigated on a low-temperature poly-silicon display panel. The GBT photosensor is formed by connection of the floating gate and body in a metal-oxide-semiconductor field-effect transistor (MOSFET). The intrinsic body region without gate metal on top is the photosensing area where the photogenerated electron-hole pairs are excited and separated. The GBT structure leads to photogenerated carrier accumulation on the floating gate and results in positive feedback of gate potential and increase of MOSFET current. Thus, the photocurrent is amplified. The photoresponse is enhanced to two to three times that of the conventional p-i-n photodiode.
© 2009 The Electrochemical Society. [DOI: 10.1149/1.3087456] All rights reserved.

Manuscript submitted January 21, 2009; revised manuscript received February 3, 2009. Published February 25, 2009.

A photosensing device fabricated using the thin-film process generally has a critical drawback of low responsivity due to its shallow substrate of ~50 nm for light absorption. The conventional p-i-n photodiode used in low-temperature poly-silicon (LTPS) process inevitably suffers from the same disadvantage. In addition, a p-i-n diode can only be realized in a complementary metal-oxide-semiconductor (CMOS) process by which both n^+ and p^+ implant steps are available. There are of course many other photodetectors with enhanced performance proposed over the years for thin-film transistor (TFT) technology.[1-3] However, most of them required additional process steps that are not fully compatible with the general TFT process for display applications. In this work, we presented an embedded photosensing structure using gate-body-tied (GBT) TFTs by the LTPS technology. A high-gain photodetector using GBT metal-oxide-semiconductor field-effect transistors (MOSFETs) based on logic CMOS technology has been reported in Ref. 4-6. The high-responsivity photosensors with a floating gate-body connection were also investigated on both silicon-on-insulator (SOI) and bulk CMOS technologies.[7,8] By extending the GBT structure to TFT technology, a high-responsivity photodetector by LTPS technology has been successfully demonstrated in this work. The GBT photosensor is realized on an LTPS display panel. The LTPS TFTs with laser-annealing crystallized poly-silicon thin films on a glass substrate exhibit a much different photoresponse from logic and SOI devices. Because of its inherent floating body, an LTPS TFT device is the best candidate in realizing a gate-body positive feedback configuration without altering the device structure and process steps. Both the characteristics of n-type and p-type GBT photosensors were studied and compared to the performance of a p-i-n photodiode. Experimental results reveal that the GBT photosensor has an increased responsivity, which is twice that of the p-i-n photodiode with the same photosensing area. The GBT photosensing structure can become a simple solution for realizing a good photosensor with p-channel metal-oxide-semiconductor (PMOS)-only LTPS technology, in which no easy-to-implement optical sensor has been available.

Sample Preparation and Measurement Setup

The investigated samples, as shown in Fig. 1, were fabricated by the standard LTPS process for display panels.[9] The H-shape of the metal gate was designed with an equal width at the sidewall to reduce the misalignment effect on the width of the active region. The ratio of the active region to the metal-covered area determines the potential of the floating node as the charge builds up under a fixed device dimension. The large photosensing area provides more photogenerated electron-hole pairs (EHPs), which results in a high photocurrent and feedback source, while a wider metal gate leads to a high MOSFET turn-on current by the feedback potential. The final output response, consisting of photocurrent and MOSFET turn-on current, should be maximized for achieving high optical responsivity while maintaining a low dark current. The photocurrents were measured with a V_{DS} bias voltage of 2.5 and −2.5 V in a GBT n-channel metal-oxide-semiconductor (NMOS) and PMOS, respectively. The samples were illuminated by a visible-spectrum white-light source ranging from 0 to 500 Lux.

As shown in Fig. 1, the GBT photodetector is composed of a TFT with the parasitic n-i-n or p-i-p structure in parallel to the transistor channel from source to drain. The exposed intrinsic regions were designed to be the photosensing area where the incident light would not be shielded by gate metal. The photogenerated EHPs are mainly separated in the drain-depletion region by its built-in potential and the applied field. For n-channel devices, electrons flow to the n^+ drain terminal and holes accumulate in the floating body, which leads to a positive potential accumulation on the floating body and gate. A positive feedback is established through the gate-body connection, which leads to high transistor channel current; hence, the amplification of photocurrent is achieved. p-Channel devices have the same amplification effect with reversed EHP motion. The p-i-n structure is similar to that of the parasitical n-i-n shown in Fig. 1b except one of the n^+ terminals was replaced by p^+ doping. The p-i-n photodiode has an identical size to GBT photodetectors for comparison.

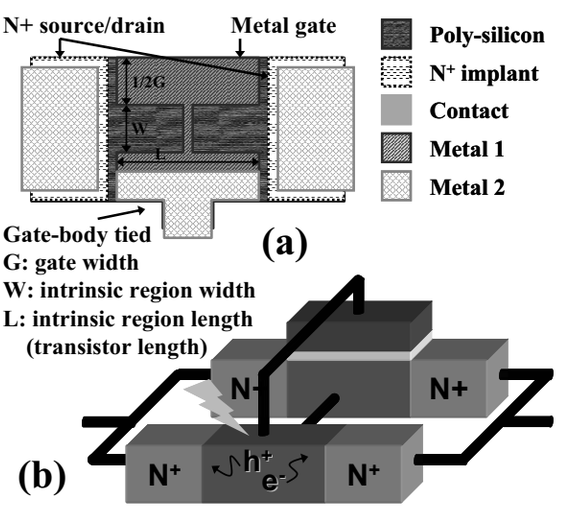

Figure 1. Layout of the photodetector by LTPS technology on a glass substrate. (b) The n-type GBT structure is equivalent to an n-channel TFT in parallel with an n-i-n structure.

[z] E-mail: wrchiang@well.ee.nthu.edu.tw

Downloaded 17 Jan 2012 to 140.114.195.186. Redistribution subject to ECS license or copyright; see http://www.ecsdl.org/terms_use.jsp

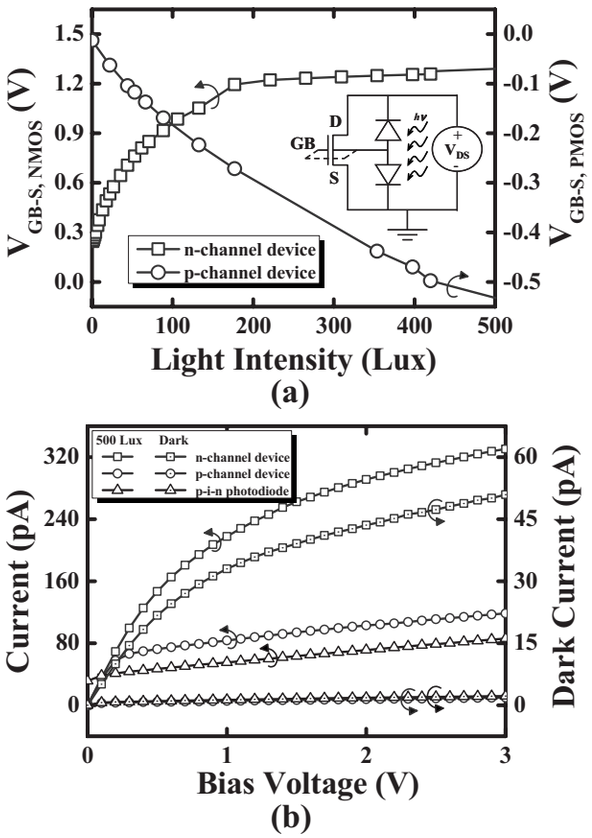

Figure 2. Potential levels of the floating gate-body nodes increase and decrease with light intensity for the n- and p-channel devices, respectively. (b) The *I-V* characteristics of both GBT devices and the p-i-n photodiode. The gate width (G), intrinsic width (W), and length are 40, 100, and 20 μm for both GBT devices, and the width and length of the p-i-n diode is 100 and 20 μm.

Results and Discussion

The voltage level of the floating gate-body node is monitored and plotted in Fig. 2a with increasing light intensity. The results present dynamic threshold voltages modulated by incident light in these transistors that would further amplify the original photocurrent, specifically under low illuminations.[10-12] Figure 2a demonstrates that the voltage level, initially at 0.5 V, of the gate-body node in the n-channel device increases with the light intensity due to the accumulation of photogenerated holes. The floating body potential increases linearly with illumination level at the low light intensity regime. Under the high-illumination situation, the source-body junction of the n-i-n bipolar structure is operated in the forward region, and the relation between the floating node potential and the photocurrent is logarithmic. Therefore, a huge amount of photogenerated EHPs accumulating in the floating node only slightly enhances the potential of the gate body. The photocurrent amplification effect is hence reduced or not as effective as the low light intensity situation. Similar behavior was found in the GBT p-channel device except with lower feedback efficiency, which might be caused by poorer contacts of the extremely slight doped body. Figure 2b shows the current-voltage (*I-V*) characteristics of the GBT devices and p-i-n photodiode. The dark current is about 10 and 0.9 times that of the p-i-n photodiode for GBT n- and p-channel devices, respectively. The current gain is about 4 and 1.5 times as compared to the p-i-n diode. Figure 3 shows the photocurrent responses of the GBT n- and p-channel devices in comparison to that of a p-i-n photodiode. The measurement results show that the photocurrent level of GBT NMOS is three to four times higher than that of the p-i-n. As discussed previously, the slight enhancement in photocurrent of the GBT PMOS is due to the poorer feedback efficiency by a p-channel implant. Figure 4 shows the dark current dependence on the width and length of each photodetector. The GBT n-channel device had a dark current almost one order larger than that of the p-i-n device. The significant dark leakage current should be as a result of a transistor operated in the subthreshold region. The dark current levels in all three devices increased with shorter channel length or intrinsic region length, which may result from the shortened leakage path. The responsivities of all three samples, as shown in Fig. 5, are all slightly enhanced with a short intrinsic region, which should be attributed to the decreased number of recombination centers in the grain boundaries. From the comparisons of photocurrents, dark currents and optical responsivities in Fig. 3-5, the GBT photodetector with enhanced photocurrent response suffered from significant degradation in dark current level. Therefore, the GBT photosensor with proper mechanisms of dark current compensation or cancellation, such as subtraction of dark reference level and correlated dual sampling, will be an attractive embedded photosensor on a LTPS display panel.[13-15]

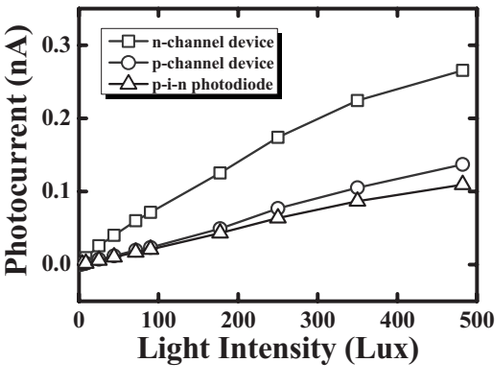

Figure 3. Photocurrent comparisons for the three devices. The gate widths (G) and intrinsic region widths (W) are 40 and 100 μm for both n- and p-channel GBT devices. The width of the p-i-n diode is 100 μm and the lengths of these three devices are all 20 μm.

Conclusion

In this article, a photodetector with amplified optical response using GBT TFT by LTPS technology is presented. The responsivity more than twice as large as that of the conventional p-i-n photodiode is achieved. Experimental results demonstrate that the GBT

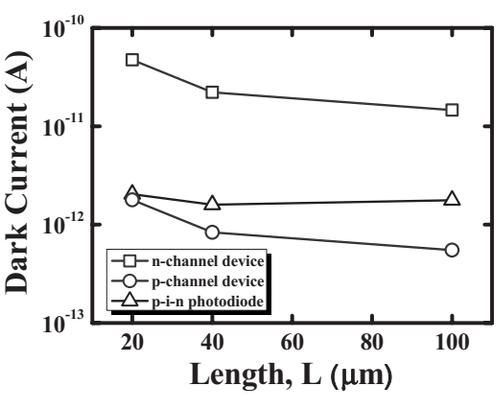

Figure 4. Dark current comparisons for samples with different lengths in intrinsic region. The gate widths are fixed at 40 μm for both the n- and p-channel GBT devices, and the widths of the three photosensing devices are all 100 μm.

Downloaded 17 Jan 2012 to 140.114.195.186. Redistribution subject to ECS license or copyright; see http://www.ecsdl.org/terms_use.jsp

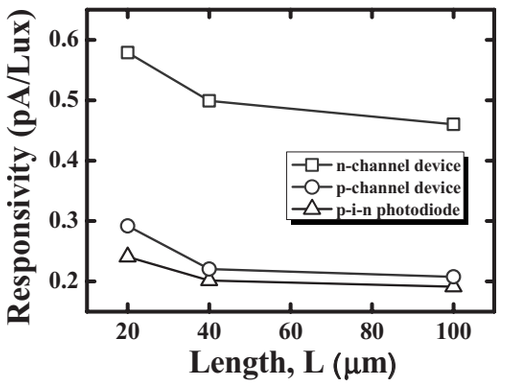

Figure 5. Optical responsivities of the n- and p-channel GBT devices and the p-i-n photodiode with different lengths of intrinsic region. The gate widths (G) are fixed at 40 μm for both the n- and p-channel GBT devices, and the widths (W) of the three photosensing devices are all 100 μm.

PMOSFET with improved feedback efficiency can be an effective and competitive solution for various photosensing applications integrated on a LTPS display panel.

Acknowledgments

The authors thank the AU Optronics Corporation for device fabrication and LTPS technology support and the National Science Council of Taiwan for funding support.

National Tsing Hua University assisted in meeting the publication costs of this article.

References

1. M. Okamura, K. Kimura, S. Shirai, and N. Yamauchi, *IEEE Trans. Electron Devices*, **41**, 180 (1994).
2. J. B. Boyce, R. T. Fulks, J. Ho, R. Lau, J. P. Lu, P. Mei, R. A. Street, K. F. Van Schuylenbergh, and Y. Wang, *Thin Solid Films*, **383**, 137 (2001).
3. E. Budianu, M. Purica, E. Manea, and M. Kusko, in *IEEE International Conference Semiconductor*, Vol. 1, pp. 151–154, IEEE, Piscataway, NJ (2003).
4. W. Zhang, M. Chan, R. Huang, and P. K. Ko, *Solid-State Electron.*, **44**, 535 (2000).
5. W. Zhang and M. Chan, *IEEE Trans. Electron Devices*, **48**, 1097 (2001).
6. J. H. Park, H. Kim, S. H. Seo, and J. K. Shin, *Opt. Rev.*, **12**, 196 (2005).
7. H. C. Chang and Y. C. King, *IEEE Sens. J.*, **3**, 525 (2003).
8. H. Yamamoto, K. Taniguchi, and C. Hamaguchi, *Jpn. J. Appl. Phys., Part 1*, **35**, 1382 (1996).
9. T. Morita, Y. Yamamoto, M. Itoh, H. Yoneda, Y. Yamane, S. Tsuchimoto, F. Funada, and K. Awane, *Tech. Dig. - Int. Electron Devices Meet.*, **1995**, 841.
10. W. Zhang, M. Chan, and P. K. Ko, *IEEE Trans. Electron Devices*, **47**, 1375 (2000).
11. K. Matsumoto, T. Nakamura, A. Yusa, and S. Nagai, *Jpn. J. Appl. Phys., Part 2*, **24**, L323 (1985).
12. K. Matsumoto, I. Takayanagi, T. Nakamura, and R. Ohta, *IEEE Trans. Electron Devices*, **38**, 989 (1991).
13. W. D. Boer, A. Abileah, P. Green, T. Larsson, S. Robinson, and T. Nguyen, *SID Int. Symp. Digest Tech. Papers*, **34**, 1494 (2003).
14. F. Matsuki, K. Hashimoto, K. Sano, D. Yeates, J. R. Ayres, M. Edwards, and A. Steer, *SID Int. Symp. Digest Tech. Papers*, **38**, 290 (2007).
15. H. Hayashi, T. Nakamura, N. Tada, T. Imai, M. Yoshida, and H. Nakamura, *SID Int. Symp. Digest Tech. Papers*, **38**, 1105 (2007).

Downloaded 17 Jan 2012 to 140.114.195.186. Redistribution subject to ECS license or copyright; see http://www.ecsdl.org/terms_use.jsp